Mantle ^{3}He distribution and deep circulation in the Indian Ocean

Ashwanth Srinivasan,[1] Zafer Top,[1] Peter Schlosser,[2] Roland Hohmann,[3]
Mohamed Iskandarani,[1] Donald B. Olson,[1] John E. Lupton,[4] and William J. Jenkins[5]

Received 2 July 2003; revised 23 February 2004; accepted 19 March 2004; published 10 June 2004.

[1] The World Ocean Circulation Experiment Indian Ocean helium isotope data are mapped and features of intermediate and deep circulation are inferred and discussed. The ^{3}He added to the deep Indian Ocean originates from (1) a strong source on the mid-ocean ridge at about 19°S/65°E, (2) a source located in the Gulf of Aden in the northwestern Indian Ocean, (3) sources located in the convergent margins in the northeastern Indian Ocean, and (4) water imported from the Indonesian Seas. The main circulation features inferred from the ^{3}He distribution include (1) deep (2000–3000 m) eastward flow in the central Indian Ocean, which overflows into the West Australian Basin through saddles in the Ninetyeast Ridge, (2) a deep (2000–3000 m) southwestward flow in the western Indian Ocean, and (3) influx of Banda Sea Intermediate Waters associated with the deep core (1000–1500 m) of the through flow from the Pacific Ocean. The large-scale ^{3}He distribution is consonant with the known pathways of deep and bottom water circulation in the Indian Ocean. *INDEX TERMS:* 4808 Oceanography: Biological and Chemical: Chemical tracers; 3319 Meteorology and Atmospheric Dynamics: General circulation; 4536 Oceanography: Physical: Hydrography; *KEYWORDS:* Indian Ocean, tracers, deep circulation

Citation: Srinivasan, A., Z. Top, P. Schlosser, R. Hohmann, M. Iskandarani, D. B. Olson, J. E. Lupton, and W. J. Jenkins (2004), Mantle ^{3}He distribution and deep circulation in the Indian Ocean, *J. Geophys. Res.*, *109*, C06012, doi:10.1029/2003JC002028.

1. Introduction

[2] Primordial helium trapped in the Earth's mantle is injected into the mid-depth ocean through submarine hydrothermal and volcanic activities. Typically, the injected helium is fivefold to tenfold enriched in the rare isotope ^{3}He compared to atmospheric helium. The injected ^{3}He is easily distinguished from the background ^{3}He signature of atmospheric origin imprinted by air-sea gas exchange. Thus the mantle ^{3}He signal can be traced over large distances in the ocean typically between 1000 and 3000 m depth. At these depths other tracer fields have no signal yet or frequently have small lateral gradients complicating their use for studies of flow patterns. ^{3}He distributions have been used successfully to infer circulation patterns in the oceans such as the westward plume in the South Pacific at 15°S [*Lupton and Craig*, 1981], the southwestward plume in the northeastern Pacific Ocean and the eastward plume from Hawaii to the Mexican Coast [*Lupton*, 1998]. These plumes clearly define the regional circulation, which is not apparent in conventional tracer fields.

[3] The first helium measurements in the Indian Ocean were obtained from the Geochemical Ocean Sections Study (GEOSECS) during 1977–1978. These were made by W. B. Clarke and Z. Top at McMaster University, J. E. Lupton and H. Craig at the Scripps Institute of Oceanography, and W. J. Jenkins at the Woods Hole Oceanographic Institution. The results revealed moderate ^{3}He enrichment with δ^3He values of 12–15% [*Östlund et al.*, 1987; *Lupton and Craig*, 1980] (δ^3He [%] = 100 × (R_{sample}/R_{air} − 1); R = ^{3}He/^{4}He). The large-scale distribution of ^{3}He is determined by the helium sources, the deep ocean circulation and ocean mixing. The GEOSECS ^{3}He measurements revealed a north-south gradient with relatively high anomalies in the northern and central Indian Ocean (δ^3He about 13–16%) and low anomaly in the southern Indian Ocean (δ^3He about 8–9%). The measurements hinted at a prominent mid-depth eastward flow in the southern Indian Ocean and influx of Pacific waters enriched in ^{3}He through the Indonesian Throughflow. The GEOSECS survey also illustrated the differences between the ^{3}He distributions in the three major ocean basins due to differences in the processes controlling its distribution. These processes include the ^{3}He injection rate and the overturning rate of the ocean basins. The deep Pacific Ocean is significantly enriched in ^{3}He (δ^3He about 25–30%) because of large-scale hydrothermal activity over the East Pacific Rise. In the Indian Ocean, δ^3He excesses are on the order of 13–15% due to moderate input and possibly faster overturning. In contrast, the deep Atlantic Ocean is least enriched in ^{3}He (δ^3He about

[1]Rosenstiel School of Marine and Atmospheric Sciences, University of Miami, Miami, Florida, USA.
[2]Lamont-Doherty Earth Observatory of Columbia University, Palisades, New York, USA.
[3]Organe consultatif sur les Changements Climatiques, ProClim-, Bern, Switzerland.
[4]Pacific Marine Environmental Laboratory, NOAA, Newport, Oregon, USA.
[5]Marine Geochemistry Department, Woods Hole Oceanographic Institution, Woods Hole, Massachusetts, USA.

0148-0227/04/2003JC002028$09.00

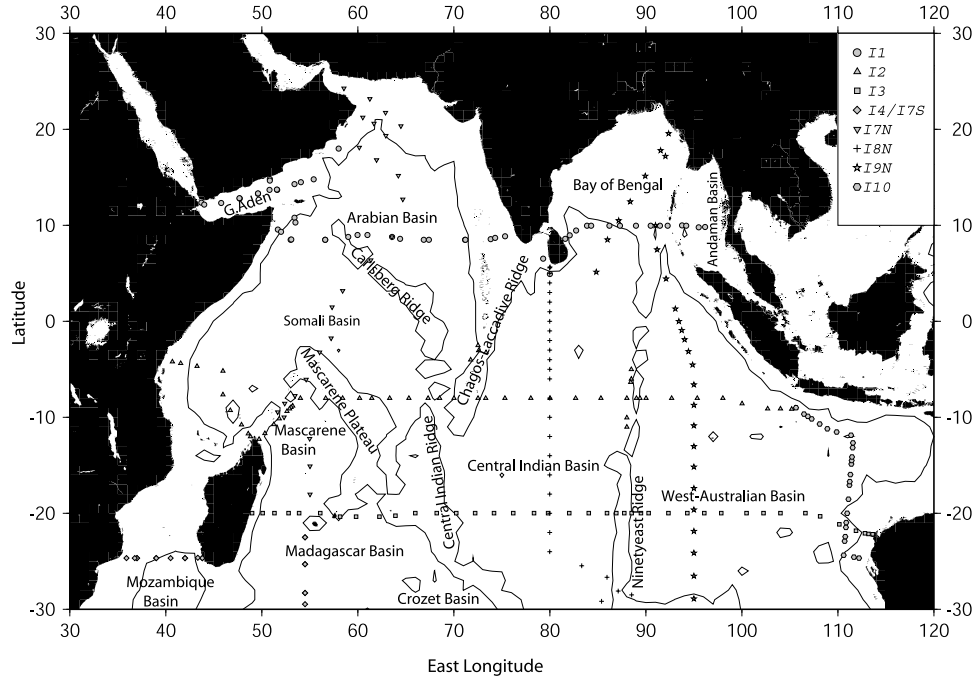

Figure 1. Index map of the Indian Ocean identifying the basin names and major topographic features. The 3500 m isobath is contoured. The symbols indicate World Ocean Circulation Experiment (WOCE) station locations where water samples were collected for helium isotope measurements.

5–8%) due to weak injection rates [*Jenkins and Clarke*, 1976; *Top et al.*, 1987; *Rüth et al.*, 2000] and relatively short turnover time [*Stuiver et al.*, 1984; *Smethie*, 1993].

[4] A decade after the GEOSECS survey the French Indigo Cruises [*Poisson et al.*, 1989] augmented the helium isotope data in the Indian Ocean. An analysis of the combined Indigo and GEOSECS helium data set by *Jamous et al.* [1992] identified the spreading centers in the Gulf of Aden, at the vicinity of the triple junction of the Central, Southeast and Southwest Indian Ridges and the Indonesian Throughflow as the main sources of mantle helium in the Indian Ocean. The resulting ^{3}He distribution revealed some features related to the characteristics of deep circulation in the Indian Ocean but could not resolve the interbasin exchanges due to the limited spatial coverage. More recent measurements in the eastern Indian Ocean and Indonesian Seas by *Jean-Baptiste et al.* [1997] and *Top et al.* [1997] indicate an influx of ^{3}He into the Indian Ocean in the 1100–1400 m depth range from the Indonesian Seas.

[5] Thus, although several features in the previously known ^{3}He distribution revealed elements of intermediate and deep circulation, there still was the need for a more complete data set that would allow derivation of the circulation patterns. To address this need the tracer component of the World Ocean Circulation Experiment (WOCE) Hydrographic Program (WHP) included ^{3}He measurements. The present analysis is based on the WOCE helium isotope data. Specifically the mantle-derived ^{3}He is mapped mainly in the 1000–3000 m depth range. Intermediate and deep circulation patterns inferred from this distribution are discussed and compared with those obtained by other means such as hydrographic and nutrients analysis [e.g., *Warren*, 1981; *Toole and Warren*, 1993; *Mantyla and Reid*, 1995; *Reid*, 2003].

2. Data and Methodology

2.1. Data

[6] The present helium isotope data are obtained from WHP lines I7N, I8N, I9N, I10, I1, I2, I3, and I4/I5W/I7S. The station locations are shown in Figure 1. Standard procedures for sampling, and sample processing were followed [*Lott and Jenkins*, 1998; *Ludin et al.*, 1998; *Clarke et al.*, 1976]. Water samples were collected in standard rosette systems equipped with 36 Niskin bottles each of volume 10 L. The samples were extracted at sea from 50 to 80 mL of water. The extracted gases were flame sealed in low-permeability glass ampoules for measurement at University of Miami (UM), Woods Hole Oceanographic Institution (WHOI), Lamont Doherty Earth Observatory (LDEO) and Pacific Marine and Environmental Laboratories (PMEL). The measurement procedures at UM, WHOI and LDEO are documented by *Clarke et al.* [1976], *Lott and Jenkins* [1998] and *Ludin et al.* [1998], respectively. The procedure followed at UM is described below and the procedures followed in the other labs are similar.

[7] The gas samples collected at sea are admitted into a processing line where gases other than helium and neon are isolated by cold trapping. A fraction of the helium and neon is routed to a quadrupole analyzer for preliminary helium and neon measurement. The remaining helium and neon is then admitted through a cryogenic trap to separate neon. Helium is finally admitted into a MAP 215-50 isotope mass spectrometer, which measures the helium isotopes. Air

Table 1. Helium Data Intercomparison Results[a]

WHP Lines[b]	Stations	Distance Apart, km	Mean Difference, %	Standard Deviation Difference, %
I1-I8N	968–284	64.5	0.4	0.3[c]
I1-I9N	987–267	120.8	0.5	0.2[c]
I1-I7N	931–782	98.4	0.5	0.4
I2-I7N	1194–740	91.8	0.7	0.7
I2-I8N	1138–322	0.4	0.1	0.4
I2-I9N	1094–190	85.9	0.2	0.3
I3-I8N	499–346	20.8	0.2	0.4
I3-I9N	471–190	112.4	0.3	0.5

[a]I1, I7 and I9N were analyzed at University of Miami, I8N was analyzed at Pacific Marine and Environmental Laboratories, and I3 and I2 were analyzed at Lamont-Doherty Earth Observatory.

[b]WHP is World Ocean Circulation Experiment (WOCE) Hydrographic Program.

[c]The I1 Rosenstiel School of Marine and Atmospheric Sciences (RSMAS) deep δ^3He were found to be systematically higher by about 1.7%. RSMAS measurements were compared with Woods Hole Oceanographic Institution measurements between depths of 1000 and 1500 m obtained at the same station. The agreement shown above is after adjustment of the RSMAS deep helium data.

samples and blanks are interspaced with the sample runs to calibrate and monitor the sensitivity changes of the instrument during operation. The precision in measurements of δ^3He data is ±0.15–0.2%. The precision in measurements of ^{4}He and total neon is about ±0.5% and ±2%, respectively.

[8] Since the helium samples were analyzed at four different labs (UM, WHOI, LDEO and PMEL) a preliminary test was performed to check for consistency between the data. This was done by comparing the helium measurements, in the depth range of 2000–4000 m at stations located close to the crossover point of any two WHP lines. The data from each station were first screened for any obvious outliers. Then a smooth spline was fitted through the data points (at least four measurements from each station were used) as a function of potential density referenced to 3000 db for each station in the crossover stations pairs identified in Table 1. For each station pair the δ^3He difference between the curves was calculated at five points that covered the density range common to the stations. The mean and standard deviation of the differences are reported in Table 1. The I1 data when compared to I7N, I9N and I8N were found to be consistently higher in δ^3He. To correct this offset we analyzed the difference between I1 samples measured by UM and WHOI at the same depth. It was found that the I1 data as measured by UM were systematically higher by about 1.7%. Therefore the I1 data used here were adjusted by subtracting 1.7%. The conclusion of this analysis is that the Indian Ocean δ^3He measurements by four different laboratories are consistent. The measurements mostly agree within ±0.2–0.4%.

2.2. Methodology

[9] The main aim of this study is to relate the observed ^{3}He distribution to large-scale circulation patterns in the deep waters of the Indian Ocean. Profiles, sections and maps of δ^3He are constructed to elucidate the distribution of ^{3}He. The results of the individual WHP lines are presented as sections and the lateral distribution is contoured on $\sigma_{1.5}$ = 34.35, σ_2 = 36.92, σ_2 = 37.00 and σ_3 = 41.495 isopycnal surfaces. These surfaces capture the features of the ^{3}He distribution at depths of roughly 1300, 2000, 2500 and 3000 m and are mostly identical with the ones used by *Mantyla and Reid* [1995] and *Reid* [2003]. The contouring on these surfaces was done by objectively mapping the data with a Gaussian covariance and a horizontal scale of 300 km. The data on the isopycnals deeper than 2000 m were first mapped within individual deep basins and then combined. The results of the objective analysis were checked by comparing with hand-contoured plots.

[10] The δ^3He maps are used to infer flow based on the spreading of the ^{3}He signal on the density surfaces. It is common in the literature to use the term "spreading" or "extending" to describe the combined effects of advection and diffusion in shaping the, steady state, property fields. However, advection is thought to be important in determining the shape of property fields [e.g., *Mantyla and Reid*, 1995; *Johnson et al.*, 1998; *Reid*, 2003]. We adopt this assumption in the discussion of ^{3}He fields. Maps of salinity, oxygen and silica on the σ_2 = 37.00 surface from *Reid*'s [2003] study are also included for reference.

[11] Before a discussion of the results a few issues warrant attention. First, the analysis presented in this study does not consider a potential source of ^{3}He to the oceans, namely, tritium decay. This decay could create a δ^3He of 5% in the thermocline depending on the location in the northern hemisphere where most of the bomb tritium was added. The low natural tritium background precludes significant tritiogenic ^{3}He in most of the deep ocean [*Jenkins and Clarke*, 1976]. Here the neglect of tritiogenic ^{3}He is reasonable because most of the tritium was added to the northern hemisphere, whereas the Indian Ocean is largely a southern hemisphere ocean, and the present discussion deals with deep waters where tritium levels have been negligible [*Östlund et al.*, 1987] even while oxygen and chlorofluorocarbons were high [*Toole and Warren*, 1993; *Fine*, 1993].

[12] Second, in describing the property fields we assume a steady state distribution. We feel that this assumption can be justified by comparing the turnover time for the deep ocean basins ($\sim 10^3$ years [e.g., *Stuiver et al.*, 1984]) with the timescale of processes controlling the mantle degassing at tectonically active sites ($\sim 10^6$ years [e.g., *Condie* 1997]). Whereas this is a reasonable assumption at global scales, it may not be necessarily true at regional scales. Indeed, *Jean-Baptiste et al.* [1997] observed anomalous ^{3}He enrichment in the eastern Indian Ocean and attributed this to transient mantle input probably associated with volcanic activity in the vicinity of the Indonesian Seas. For the present discussion, the ^{3}He distribution is considered to be in steady state in the absence of any noticeable anomaly, which would suggest otherwise.

[13] Finally, the abyssal Indian Ocean is divided into five major basins by a complex ridge system (Figure 1) [*Fisher et al.*, 1982]. This ridge system severely constrains the path of bottom water circulation but is either nonexistent or extremely porous at the depth levels discussed in this study. Nevertheless, for most part of the following discussion it is convenient to divide the deep Indian Ocean into five different basins following the 3500 m isobath. It is well known that bathymetry exercises control on flow patterns and mixing even if there is no physical barrier by a ridge system. Flow patterns often follow bathymetric features that are located several thousand meters deep in the water column [e.g., *Toole and Warren*, 1993; *Toole et al.*, 1994].

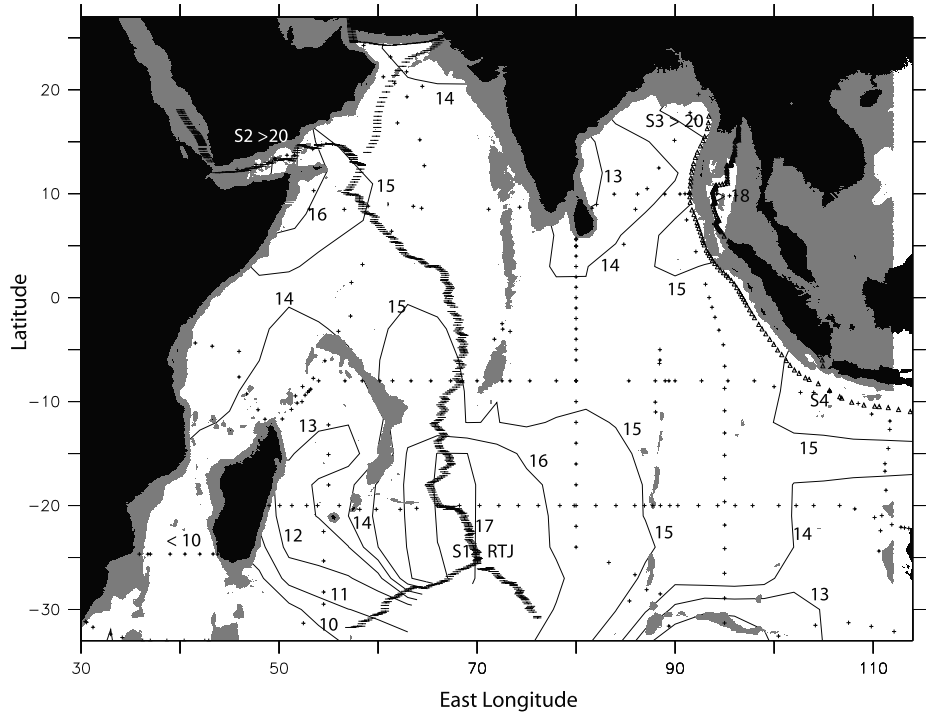

Figure 2. Map of maximum δ^3He [%] measured at each station during WOCE. The four main source areas are marked S1 thorough S4 and are described in the text. The present-day plate boundaries from *Coffin et al.* [1998] are also shown. (Dashes represent Ridge spreading centers, and triangles represent Convergent Plate Margin; RTJ is Rodriguez Triple Junction.)

Therefore these basins are constantly referred to, while discussing the ^{3}He distribution and inferring flow directions although they may not be physically present as a distinct entity.

3. Results

3.1. Mantle ^{3}He Sources in the Indian Ocean

[14] A map of maximum δ^3He values observed during WOCE at each sampling location is shown in Figure 2. Four regions of elevated δ^3He (marked S1 through S4) corresponding to the source areas of mantle ^{3}He are seen in this map. Also included in this map are the present-day plate boundaries from *Coffin et al.* [1998]. From this map it is seen that two sources are located on the mid-ocean ridge systems and two sources are located in the convergent margins in the eastern Indian Ocean and Indonesian Seas.

[15] The strongest source is the mid-ocean ridge source located at roughly 19°S, 67°E on the spreading center in the vicinity of the triple junction of the Central, Southwestern and Southeast Indian Ridges (marked as S1 in Figure 2 [*Jean-Baptiste et al.*, 1992]). The effects of this source are mainly seen in the southeastern Indian Ocean centered at a depth of 2500 m (Figure 3a).

[16] Another strong source is located in the spreading center located within the Gulf of Aden in the northwestern Indian Ocean at roughly 12°N, 45°E (marked as S2 in Figure 2). This source was identified previously by *Jean-Baptiste et al.* [1990]. Mixing and outflow from the Gulf of Aden transports ^{3}He from the source region into the Indian Ocean. The ^{3}He enrichment due to this source is mainly confined to the western Indian Ocean. The maximum anomaly observed is 22.6% at a depth of 2200 m (Figure 3b). It is also the maximum anomaly observed in the deep Indian Ocean during WOCE.

[17] Regional ^{3}He enrichment observed in the northeastern Indian Ocean (marked as S3 in Figure 2) reveals a third ^{3}He source. Profiles from this region show ^{3}He enrichment in the 1500–2000 m depth range (Figure 3c). The maximum anomaly in the eastern Indian Ocean is in the Bay of Bengal region (δ^3He > 20%). Anomalies as large as 19% are also found within the Andaman Basin which is a tectonically active back arc basin.

[18] Finally, elevated δ^3He values (maximum ~16%) observed at depths between 1000 and 1500 m in the Indonesian Throughflow region point to an indirect source of ^{3}He to the Indian Ocean (Figure 3d). The origin of this ^{3}He is a combination of both mid-ocean ridge derived ^{3}He in the Pacific Ocean and additional input in the Indonesian Seas. The ^{3}He rich deep Pacific waters enter the Indonesian Seas and pass through a series of deep basins before entering the Indian Ocean [e.g., *Gordon et al.*, 2003]. While in transit in the Indonesian Seas they are further enriched in ^{3}He by local sources [*Jean-Baptiste et al.*, 1997; *Top et al.*, 1997]. The deep component of the through flow transports this ^{3}He into the Indian Ocean.

[19] The ^{3}He/^{4}He ratios of the injected helium from the above regions are shown in Figure 4. The ratios were calculated based on a recent method developed by *Roether et al.* [1998]. The ^{3}He/^{4}He ratios of the injected helium reveal distinct differences between the individual sources in the Indian Ocean. The ^{3}He/^{4}He ratio in the vicinity of the

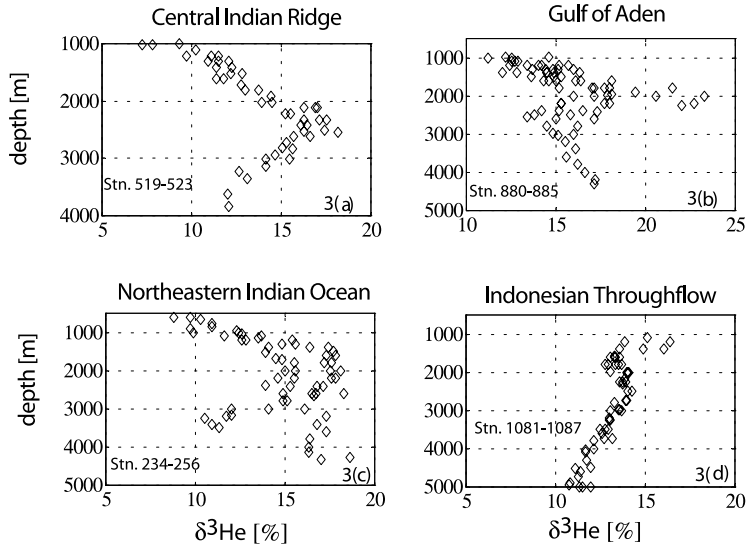

Figure 3. Profiles of δ^3He [%] in the vicinity of the sources. The location and station numbers are indicated on the plots.

Central Indian Ridge source is approximately 8–9 times the atmospheric ^{3}He/^{4}He ratio of 1.38×10^{-6}. This is typical of mantle helium. Similar ratios have been observed at hydrothermal vents on mid-ocean ridge spreading centers [*Craig and Lupton*, 1981]. The ^{3}He/^{4}He ratios from the Gulf of Aden and the northeastern Indian Ocean are approximately 5 and 3 times the atmospheric ratio, respectively. Both these ratios are significantly lower than isotopic ratio of helium derived from the mantle. It is difficult to comment on the origin of this difference without a detailed analysis since the differing solubility of helium at different locations could create spurious results. However, if the difference is real the low ratios suggest a source of crustal helium. Low ratios of ^{3}He/^{4}He have been observed before in similar tectonic

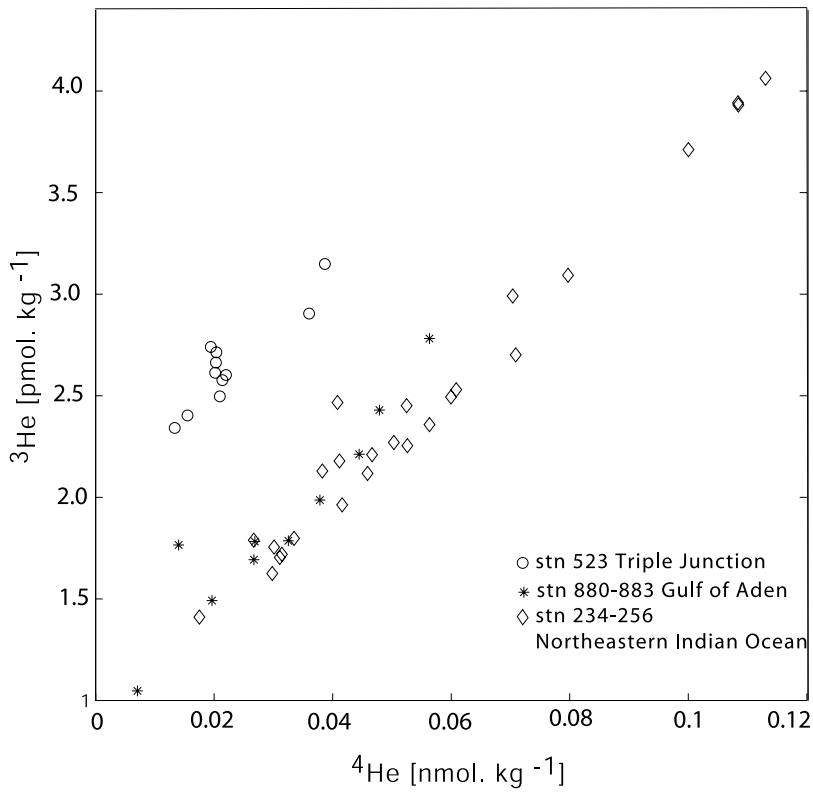

Figure 4. Plot of ^{3}He versus ^{4}He for source regions in the Indian Ocean. The difference in the slopes is discussed in the text.

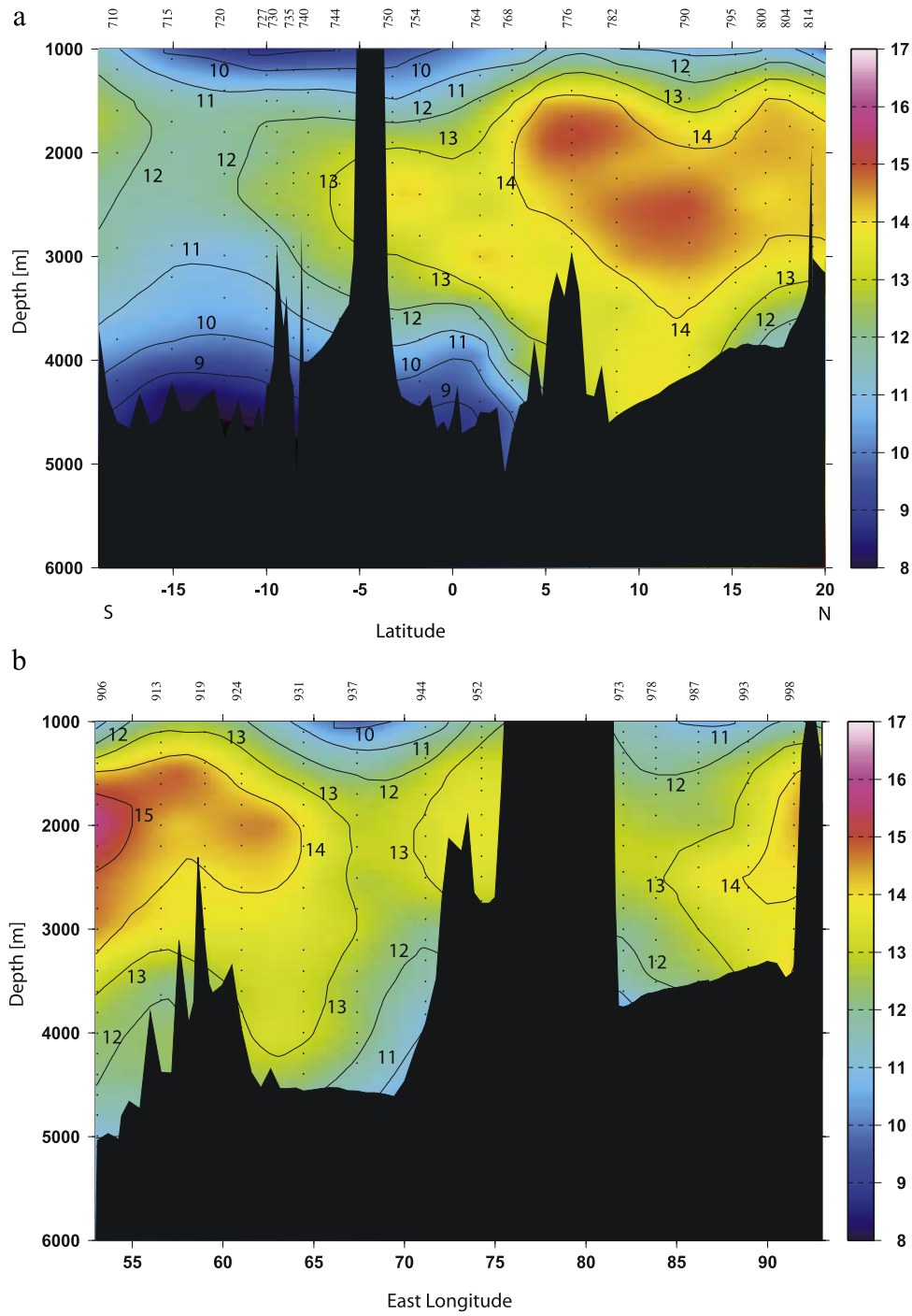

Figure 5. Vertical sections of δ^3He [%] in the Indian Ocean: (a) I7N along approximately 60°E, (b) I1 along approximately 8°N, (c) I3 along approximately 20°S, (d) I2 along approximately 8°S, (e) I8N along approximately 80°E, and (f) I9N along approximately 95°E. The dots represent sample locations at each station identified by station numbers on the top of the plot.

settings and it has been attributed to a flux of ^{4}He from the crust and sediments [*Belviso et al.*, 1987].

3.2. ^{3}He Distribution

3.2.1. Western Indian Ocean

[20] WHP Line I7N (Figure 5a) captures the ^{3}He distribution in the western Indian Ocean. ^{3}He anomalies (δ^3He > 14%) originating from the source located at the Gulf of Aden can be seen spreading southward from the western Indian Ocean in the 1500–3500 m depth range. This southward spreading is well correlated with other water properties which show a general southward movement of Indian Deep Water (IDW) in the 2000–3500 m depth range [e.g., *Wyrtki*, 1971; *Spencer et al.*, 1982; *Mantyla and Reid*,

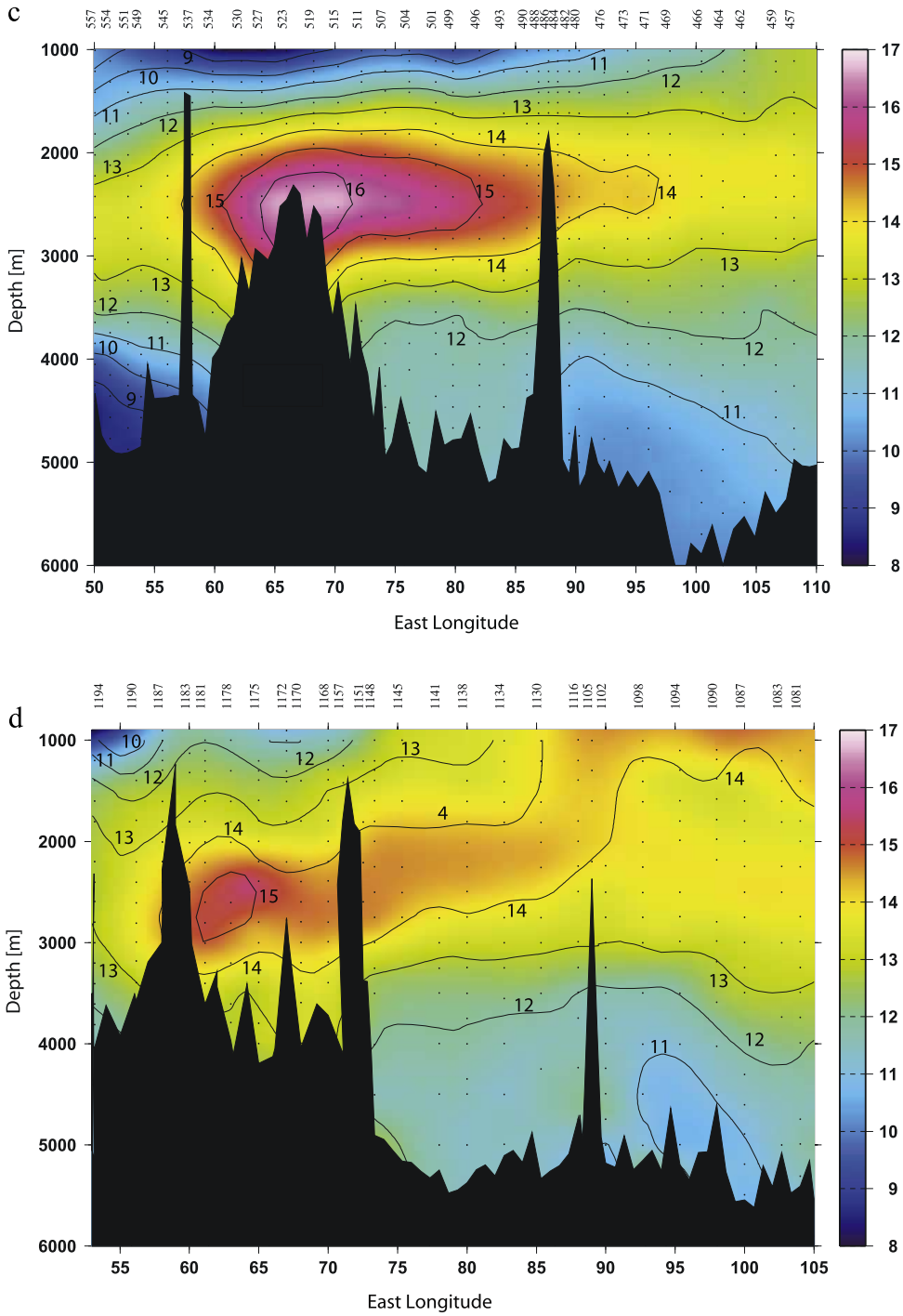

Figure 5. (continued)

1995; *Reid*, 2003]. While this pattern was previously known from the GEOSECS and INDIGO data [*Jamous et al.*, 1992], the new data show much greater detail in this region.

[21] In order to discuss the ^{3}He distribution in the northwestern Indian Ocean it is convenient to refer to parts of the Arabian and Somali Basins north of the equator as the Arabian Sea following *Warren and Johnson* [1992]. In the deep Arabian Sea, higher ^{3}He enrichment is found farther to the south at the western boundary than in the interior. Maps of δ^3He on σ_2 = 36.92, σ_2 = 37.00 and σ_2 = 41.495 isopycnal surfaces roughly at 2000 m, 2500 m and 3000 m depths, respectively (Figures 6b, 6c, and 6d), reveal a southwestward spreading of the ^{3}He signal along the western boundary of the deep Arabian Sea. This is clearly seen in the ^{3}He distribution on the σ_2 = 37.00 surface, which shows δ^3He values in excess of 14% close to the African Coast as far south as 10°S (Figure 6c). This indicates the presence of a southwestward flowing Deep Western Boundary Current (DWBC) in this region reported by several authors [e.g., *Fieux et al.*, 1986; *Dengler et al.*, 2002]. The

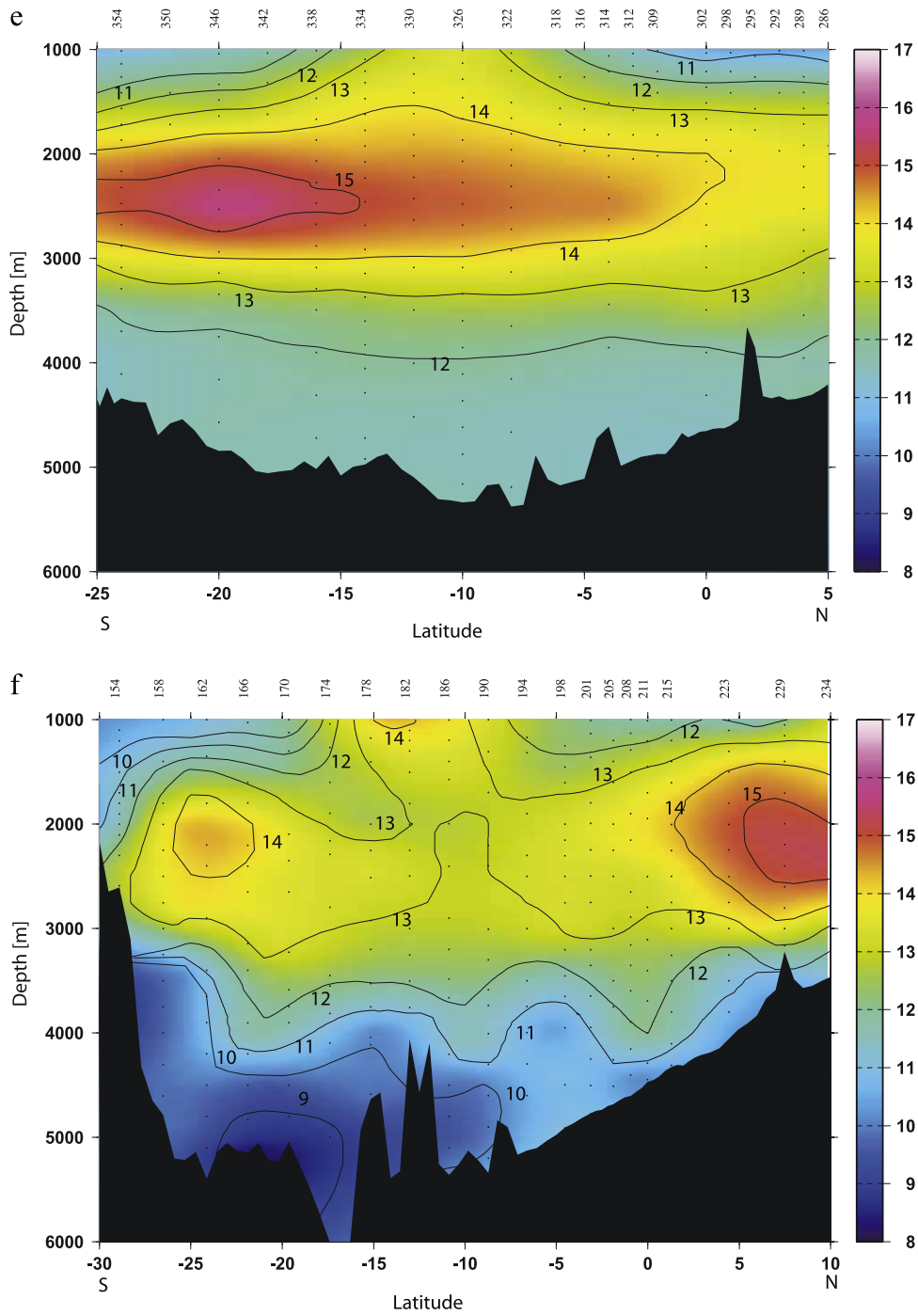

Figure 5. (continued)

southward flow close to the African Coast appears to be stronger at 2500 and 3000 m than at 2000 m since the ^{3}He enrichment at 10°S is higher at these depths than at 2000 m, while the maximum enrichment near the Gulf of Aden is between 1700 and 2200 m. This southwestward spreading is associated with similar southwestward extending high-salinity (34.75–34.80), low-oxygen (140–160 μmol kg^{-1}) and high-silica (130–140 μmol kg^{-1}) tongues in the western Indian Ocean. These features are clearly seen in *Mantyla and Reid* [1995] and *Reid*'s [2003] property maps on the σ_2 = 37.00 surface (Figures 7a, 7b, 7c and 7d).

[22] In the interior Arabian Sea there is a thick layer (1500–3500 m) of water with high ^{3}He anomalies (δ^3He > 14%) north of 10°N which extents eastward to approximately 65°E (Figures 5a and 5b). South of 10°N the Carlsberg Ridge limits the vertical extent of this layer to a depth range between 1500 and 2500 m. From Figures 5a and 5b it is also seen that the bottom waters in the interior Arabian Basin have higher ^{3}He than the bottom waters in the interior northern Somali Basin.

[23] South of the equator, in the interior Somali Basin, the ^{3}He distribution shows a three-layer structure (Figure 5a).

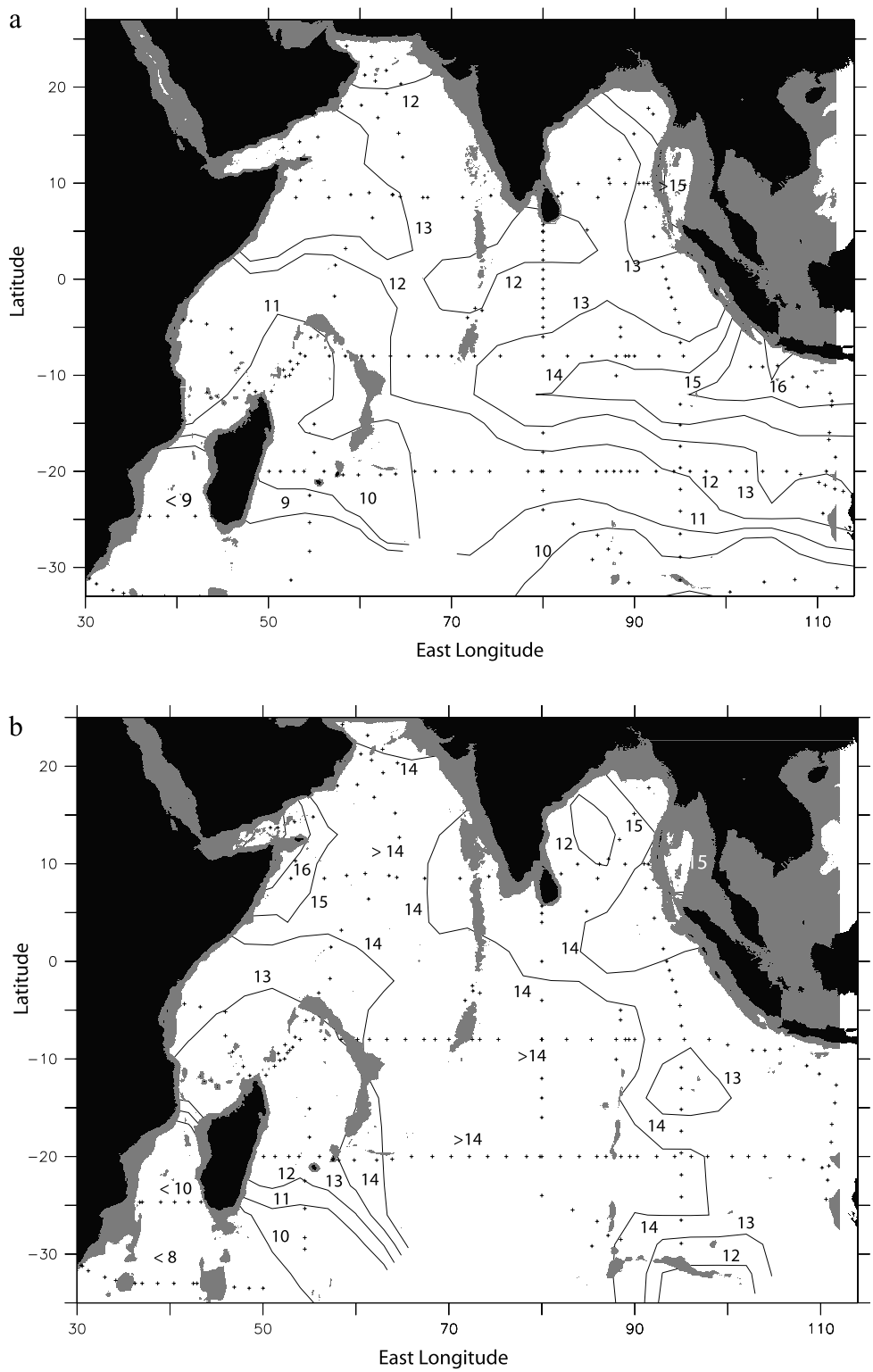

Figure 6. Map of the δ^3He [%] distribution on (a) $\sigma_{1.5}$ = 34.35 isopycnal surface, with 1500 m isobath contoured; (b) σ_2 = 36.92 isopycnal surface, with 2000 m isobath contoured; (c) σ_2 = 37.00 isopycnal surface, with 2500 m isobath contoured; (d) σ_3 = 41.495 isopycnal surface, with 3000 m isobath contoured. Data locations are marked with plus signs.

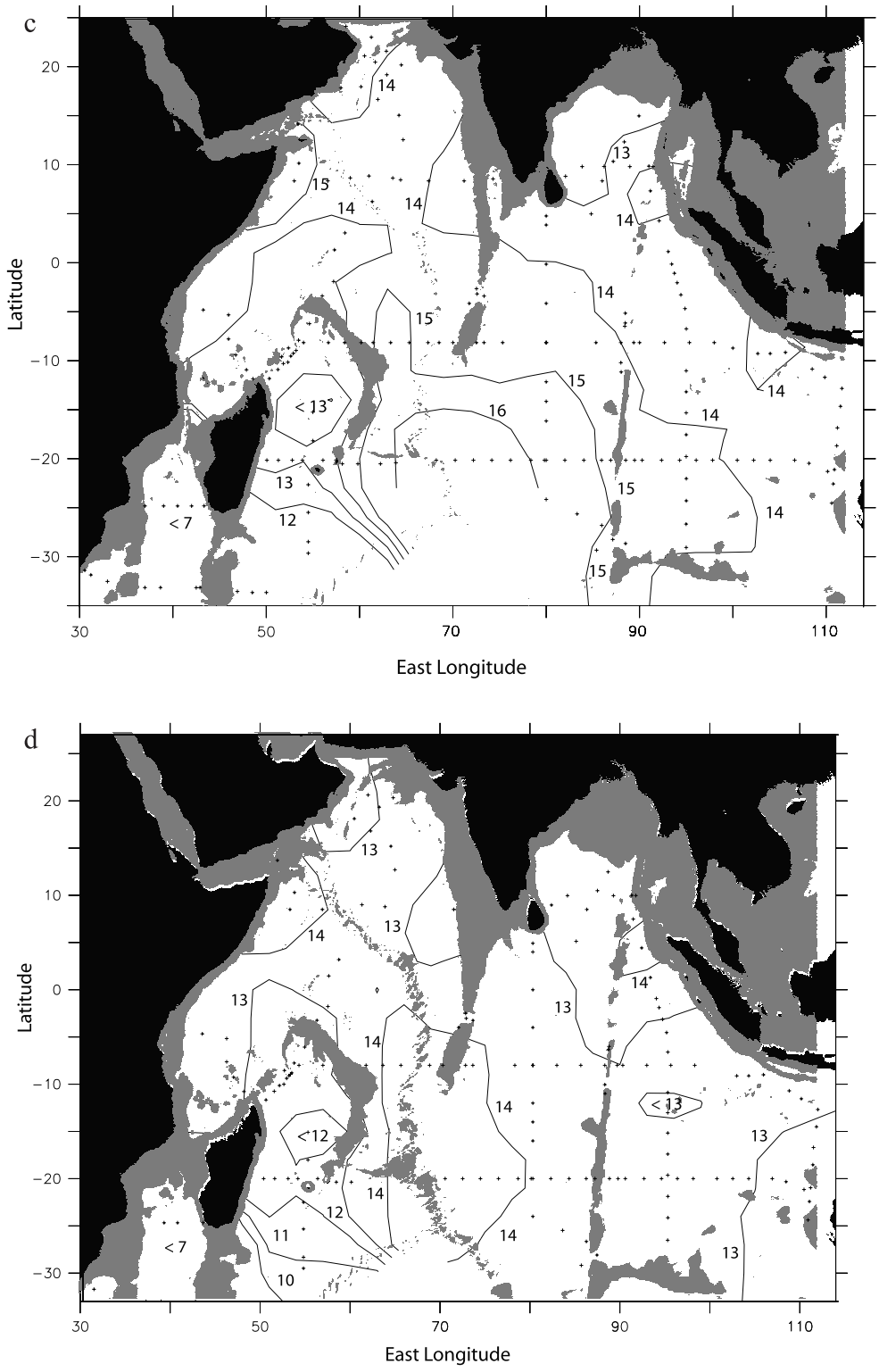

Figure 6. (continued)

The waters in the depth range of 2000–3000 m are significantly enriched (δ^3He > 13%) indicating continuation of southward spreading noted previously. Above the bottom water but below the nominal height of the Carlsberg Ridge (~3000 m) the waters are moderately enriched in ^{3}He (δ^3He about 11–13%), probably due to mixing with waters above. The bottommost waters are characterized by δ^3He values around 10%. In this layer potential temperature ranges between 0.9°C and 1.20°C, salinity is relatively low (about 34.72), oxygen values are fairly high (>175 μmol kg^{-1}) and

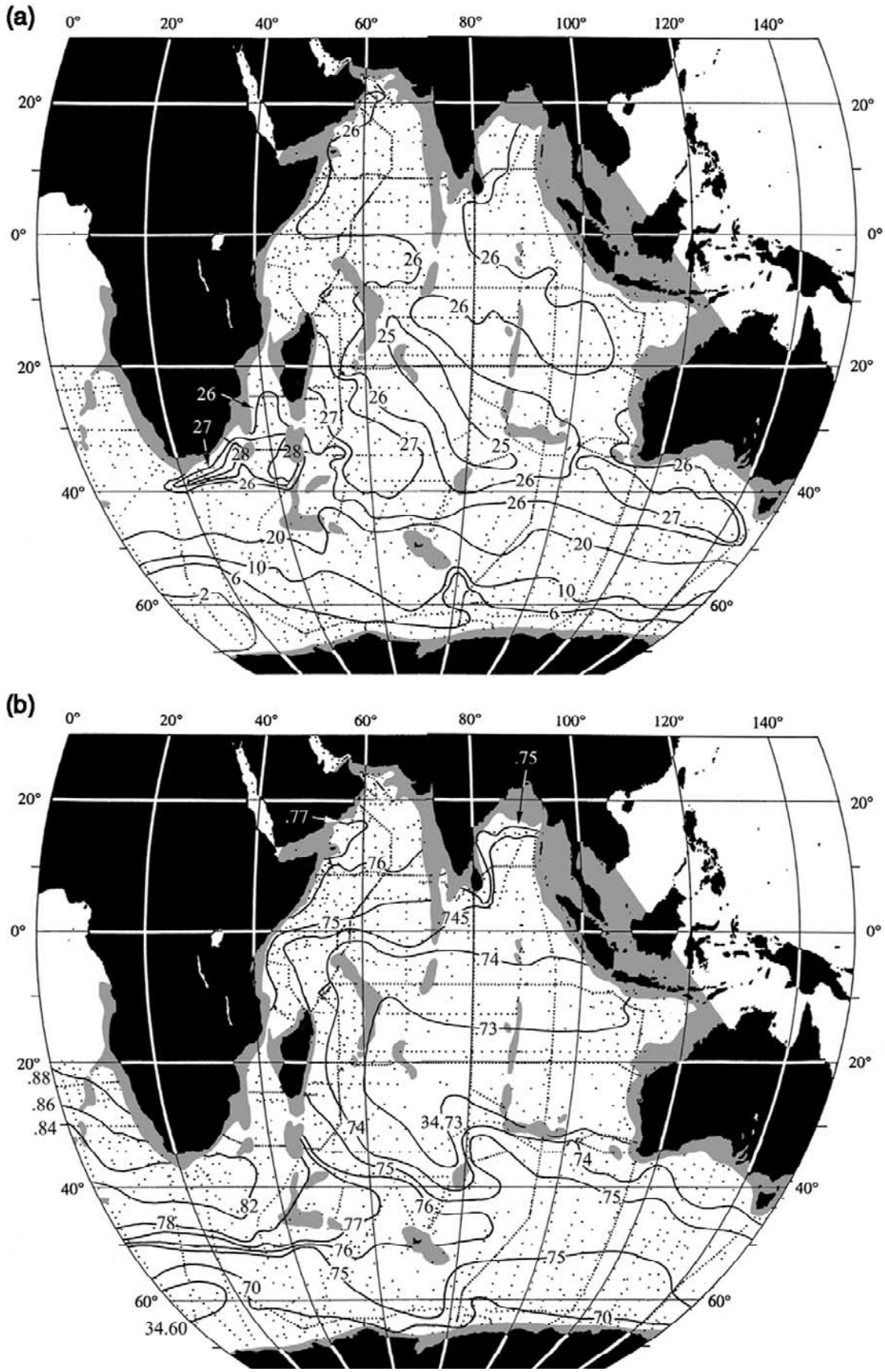

Figure 7. Maps (reprinted from *Reid* [2003] with permission from Elsevier) of hydrographic properties on σ_2 = 37.00 isopycnal surface defined by 37.00 in σ_2: (a) depth (hm), (b) salinity, (c) oxygen (ml L^{-1}), and (d) silica (μmol kg^{-1}).

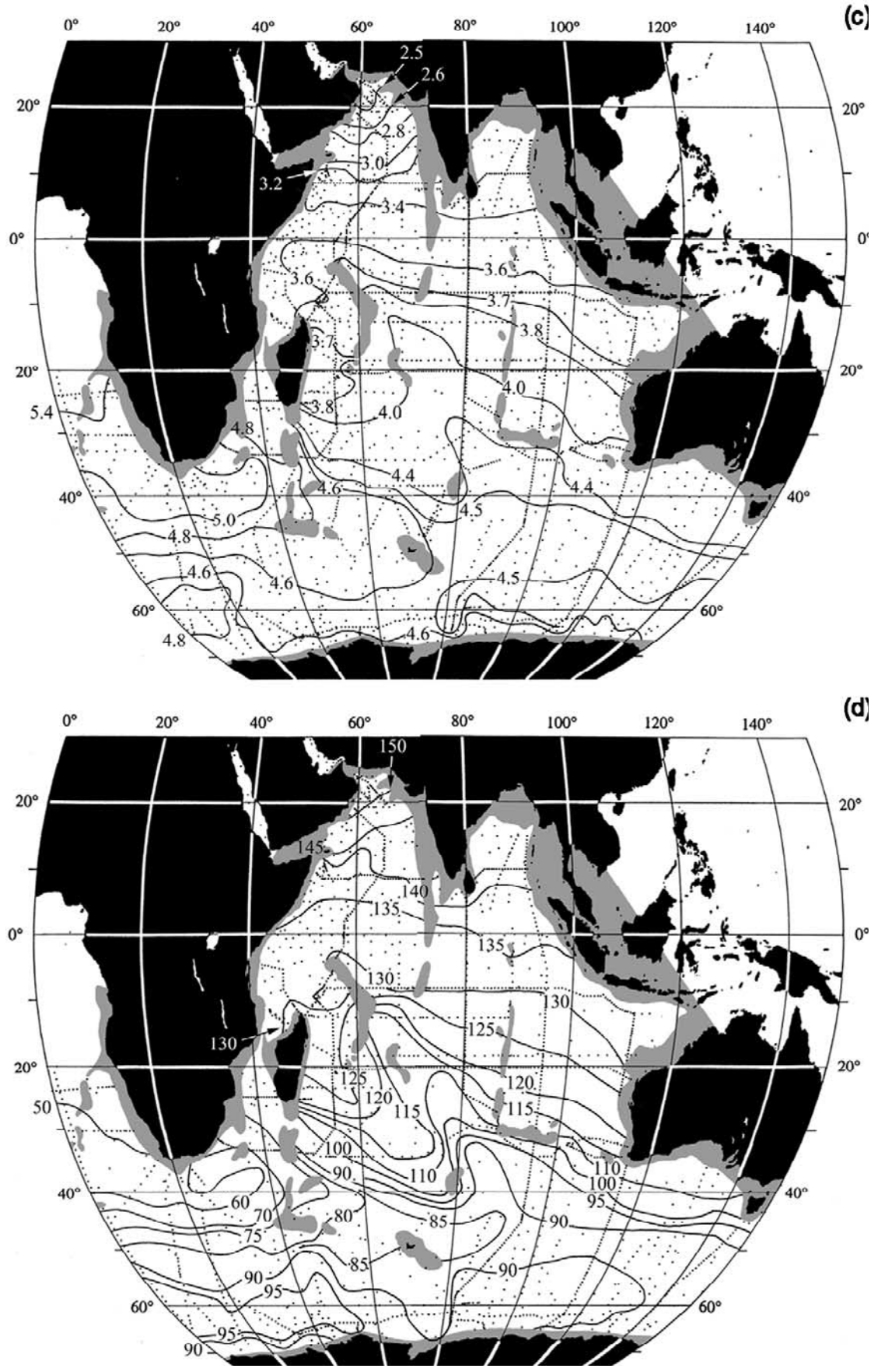

Figure 7. (continued)

silica values range between 125 and 130 μmol kg^{-1}. The low ^{3}He content and the hydrographic characteristics of these waters are typical of northward flowing Circumpolar Deep Water (CDW) supplying bottom water to the Somali Basin.

[24] East of 60°E the ^{3}He anomaly in the southern Somali Basin is relatively high and is greater than 14% (Figures 6c and 6d). The high ^{3}He content is associated with relatively low salinity ($\Delta S \sim -0.01$) and higher oxygen ($\Delta 0_2 >$ +5 μmol kg^{-1}) concentrations (Figures 7b and 7c). This is due to a northwestward inflow of ^{3}He-enriched waters from the boundary current at these depths in the Central Indian Basin. This boundary current inflow was first reported by *Warren* [1981, 1982] and is well supported by observations [*Wyrtki*, 1971; *Mantyla and Reid*, 1995; *Dengler et al.*, 2002; *Reid*, 2003]. A tongue of relatively fresh and oxygen-rich water along the northeastern flank of the Mascarene Plateau can clearly be seen in Reid's maps (Figures 7b and 7c). In this depiction it also appears that this current is a part of the boundary current of the eastern flank of the Central Indian Ridge. The ^{3}He anomaly in the vicinity of this current in the Central Indian Basin is >15%. The anomaly east of 60°E, close to the Mascarene Plateau is also >15%, which agrees well with the inflow of boundary current waters from the Central Indian Basin. However, the fate of this water in the Somali Basin is not very clear. In the southern Somali Basin between the ^{3}He enrichment in the east due to the above inflow and the ^{3}He enrichment farther west due to the southwestward flow is a region of relatively low ^{3}He enrichment extending northward from the Mascarene Plateau to the equator. This low-^{3}He region was first noted by *Jamous et al.* [1992]. It is possible that the ^{3}He-enriched inflow from the east mixes with the ^{3}He poor waters and the ^{3}He signal is quickly diminished to surrounding values.

[25] The WHP line I7N covers the Amirante Passage and the Mascarene Basin meridionally, whereas the line I2 sampled the northern boundary of this basin zonally. The waters between 2000 and 3000 m are moderately enriched (δ^3He about 12–13.5%) in the northern Mascarene Basin close to the Amirante Passage (Figures 5a and 5d). Again this is likely to be the continuation of the southward spreading water originating in the Arabian Sea. This suggests that the IDW from the deep Arabian Sea region is transported south through the gap between Madagascar Island and the Mascarene Plateau via the Amirante Passage. This is in good agreement with observations of IDW at 18°S in the Mascarene Basin by *Warren* [1981]. The northern Mascarene Basin (8°S to 10°S) appears to mark the southern limit of the helium signal originating in the Gulf of Aden. In the interior Mascarene Basin between 10°S and 15°S the ^{3}He anomaly is relatively low (δ^3He < 13%) on the σ_2 = 36.92, σ_2 = 37.00 and σ_2 = 41.495 isopycnal surfaces (Figures 6b, 6c and 6d) which indicates influence of water of southern origin.

[26] The waters deeper than 3500 m in the Mascarene Basin are very uniform and have low ^{3}He content (δ^3He < 10%) at all stations in this basin. The low ^{3}He content at depths greater than 3500 m is due to the inflow of waters of circumpolar origin. Numerous studies have observed CDW flowing northward close to the Madagascar Coast in this basin [e.g., *Warren,* 1981; *Mantyla and Reid*, 1995; *Johnson et al.*, 1998]. The relatively low ^{3}He anomaly of these waters is similar to observations farther south in the circumpolar waters by *Jean-Baptiste et al.* [1991].

[27] Farther south in the Madagascar Basin the main feature is the westward spreading ^{3}He anomaly centered on the σ_2 = 37.00 surface at 20°S seen in the I3 section (Figures 5c and 6c). This westward spreading anomaly originates from the source located on the Central Indian Ridge probably due to isopycnal mixing. It appears to be limited to a very narrow zone of less than 4° meridional extent since the ^{3}He enrichment measured at stations 710 and 700 at 18°S and 22°S during I7N and I7S is lower by almost 2%. At greater depths the bottom waters in this basin are characterized by low ^{3}He content with δ^3He of 7–8% typical of Circumpolar Deep Waters that ventilate the abyssal Indian Ocean.

[28] In the southwest corner of the Indian Ocean, in the Mozambique Basin, the δ^3He values are the lowest measured anywhere in the Indian Ocean. The δ^3He values are on the order of 6–9%. The low ^{3}He content of the deep waters of this basin is mainly due to the influence of ^{3}He-poor North Atlantic Deep water that fills this deep basin [*Toole and Warren*, 1993; *Mantyla and Reid*, 1995; *Reid*, 2003].

3.2.2. Central and Eastern Indian Ocean

[29] The WOCE Line I3 is a zonal section cutting across the Central Indian Basin along 20°S (Figure 5c). A mid-depth eastward spreading ^{3}He anomaly is strikingly visible in this section. The eastward extending tongue of ^{3}He anomaly is clearly seen emanating from the Central Indian Ridge (65°E and 2500 m). The anomaly spans the Central Indian Basin and spills into the West Australian Basin by overflowing through saddles in the Ninetyeast Ridge. An envelope of δ^3He values greater than 14% at 2000–3000 m depth range is clearly seen in the I9N section (Figure 5f) and extends to about 100°E. This indicates a strong deep eastward flow and is in very good agreement with the recent discovery of eastward flow from the Central Indian Basin into the West Australian Basin at 28°S in the depth range between 2000 and 3400 m by *Warren and Johnson* [2002].

[30] Farther north, at 8°S, at depths of 2000–3500 m higher ^{3}He enrichment is found in the trough between the Central Indian Ridge and the Mascarene Plateau than in the Central Indian Basin (Figure 5d). This suggests that the most of the DWBC flowing northward along the Central Indian Ridge [*Warren*, 1981, 1982] branches into a northwestward flowing DWBC along the Mascarene Plateau supplying water to the southern Somali Basin as noted previously.

[31] In the Central Indian Basin the main feature is a 1000 m thick layer with δ^3He > 14% that shoals upward eastward. *Warren and Johnson* [2002] have inferred westward inflow of waters from the West Australian Basin into the Central Indian Basin at 10°S and 5°S in the 2000–3500 m depth range. The ^{3}He data in the vicinity of the Ninetyeast ridge at the overflow latitudes do not provide unambiguous evidence for overflow but the effects of this westward mid-depth flow are also seen in the I2 section. The shoaling of the lower 14% isopleth from 3500 m at the Central Indian Ridge to approximately 2200 m near the Ninetyeast Ridge is likely due to the inflow mentioned above. Additional indication of the branching of the DWBC

westward and westward flow comes from the ^{3}He distribution along 80°E in the Central Indian Basin (Figure 5e). In this section the ^{3}He anomaly of magnitude greater than 15% extends to about 12°S which is the approximate latitude of branching and the westward inflow from the West Australian Basin. The absence of ^{3}He enrichment greater than 15% in the Central Indian Basin north of this latitude is consonant with the branching of the DWBC and westward inflow from West Australian Basin. The extent of the mid-depth ^{3}He anomaly, the eastward flow in the Southern Central Indian Basin and the branching of the DWBC are clearly visible in maps of δ^3He on σ_2 = 36.92, σ_2 = 37.00 and σ_3 = 41.495 isopycnal surfaces (Figures 6b, 6c and 6d). In the region of the ^{3}He maximum, potential temperature ranges between 1.5°C and 1.6°C while salinity and oxygen are in the range of 34.72–34.73 and 170–175 μmol kg^{-1}, respectively. The ^{3}He anomaly north of the equator is about 13.5% compared to about 14.5% south of the equator.

[32] In the northeastern Indian Ocean, high ^{3}He anomalies (δ^3He about 15%) can be seen spreading southward from the Bay of Bengal region in the 1500–3000 m depth range (Figure 5f). This high ^{3}He anomaly is due to sources located in the convergent margins discussed above and the southward spreading is probably due to mixing. Within the Bay of Bengal region (Figure 5a) the ^{3}He anomaly decreases from east to west with a pronounced westward spreading near the bottom. Direct measurements in this region suggest an anticlockwise near bottom flow in this region [*Gordon et al.*, 2002]. The ^{3}He distribution is consistent with this circulation scheme.

[33] The bottom water in the Central Indian Ocean (δ^3He about 12%) is relatively enriched compared to the bottom waters in the western and eastern Indian Ocean (δ^3He about 9%). This distribution illustrates the unique deep circulation in this basin. The bottom waters deeper than 3800 m are derived from the West Australian Basin through saddles in the Ninetyeast Ridge at 10°S and 5°S [*Warren*, 1981, 1982; *Warren and Johnson*, 2002]. Therefore the bottom waters of the Central Indian Basin should have greater ^{3}He enrichment than both the western and eastern basins since the bottom waters in the latter two basins are derived directly from the ^{3}He depleted southern ocean waters, whereas the bottom water in the Central Indian Ocean have been enriched by mixing during transit through the West Australian Basin.

[34] Bottom water in the West Australian basin has a relatively low anomaly, indicating inflow of Circumpolar Deep Water (Figures 5c, 5d and 5f). This low-δ^3He layer is thickest south of 10°S. Bottom water north of 10°S is relatively enriched in ^{3}He due to the mixing with ^{3}He rich waters above. In the West Australian basin the least enriched waters are found close to the eastern flank of the Ninetyeast Ridge in the region of the boundary current transporting ^{3}He poor bottom waters northward (Figure 5c). Farther east this low-^{3}He anomaly layer is less thick suggesting recirculation and southward flow of relatively ^{3}He rich waters in the eastern part of the basin. This agrees well with other descriptions of abyssal flows in this region [*Warren*, 1981; *Mantyla and Reid*, 1995].

[35] At intermediate depths (1000–1500 m) in the latitude range of 5°S–15°S the ^{3}He enrichment associated with the deep through flow from the Indonesian Seas is clearly discernable in the sections along 8°S, 95°E, 80°E and the δ^3He map on the $\sigma_{1.5}$ = 34.37 surface (Figures 5d, 5e, 5f and 6a). This ^{3}He enrichment is associated with the influx of ^{3}He rich intermediate depth relatively fresh water from the Banda Sea known as Banda Sea Water or Banda Sea Intermediate water [e.g., *Wyrtki*, 1961; *Rochford*, 1966; *Warren*, 1981; *Wijffels et al.*, 2002]. The ^{3}He anomaly due to this through flow is on the order of 14–15% close to the eastern boundary of the Indian Ocean. The δ^3He map on $\sigma_{1.5}$ = 34.37 surface at roughly 1300 m shows the extent of the ^{3}He input from the Indonesian Seas. The core of the ^{3}He signal is observed to spread westward between at 10°S and 12°S from the eastern Indian Ocean to about 70°E. The ^{3}He maximum is associated with a potential temperature range between 4.7°C and 5.0°C going from east to west along this isopycnal. Salinity and oxygen are less than 34.70 and 90 μmol kg^{-1}, respectively.

4. Discussion and Conclusions

[36] The vastly improved coverage obtained from the new measurements point out several interesting features of the nature of the ^{3}He sources in the Indian Ocean. While the source areas of ^{3}He were generally known from previous measurements, their strength and nature were not well known. Perhaps the most interesting result with respect to the sources is that the deep Indian Ocean receives input from sources both within and outside the Indian Ocean. Among the sources within the Indian Ocean are two essentially point sources located on the mid-ocean ridges and several distributed sources in the convergent margins in the eastern boundary. The deep core of the Indonesian Throughflow brings ^{3}He into the Indian Ocean from sources located in the Pacific Ocean and the Indonesian Seas. This unique distribution of sources in the Indian Ocean has important implications for modeling studies using ^{3}He. These studies require a source function for the release of ^{3}He into the deep ocean. For example, in one of the first attempts to simulate the global oceanic ^{3}He distribution, *Farley et al.* [1995] linked a simple mid-ocean ridge source function to an oceanic general circulation model. The source function used in this study assumed an even distribution of sources along mid-ocean ridges only. Because of lack of evidence they did not include sources of ^{3}He other than mid-ocean ridge spreading centers. As results from new data demonstrate, the assumption of uniformly located sources may not be appropriate in the Indian Ocean. The new data can be used to construct a more accurate source function.

[37] Another important result with respect to sources is the contribution of convergent margins to the Indian Ocean. The northeastern boundary of the Indian Ocean is a convergent margin associated with the Sunda Arc extending from the Indonesian Seas into the Bay of Bengal region (Figure 2). Here the Indian and the Australian Plates are subducted under the Eurasian Plate and this is a region of active volcanism [*Condie*, 1997]. Transient releases of energy and mantle volatiles have been observed at submarine volcanic areas at convergent margins [*Belviso et al.*, 1987]. The observed anomaly in the eastern Indian Ocean suggests that convergent margins are a significant source of mantle ^{3}He to the Indian Ocean. However, to quantify the contribution of convergent margins to the ^{3}He budget in the

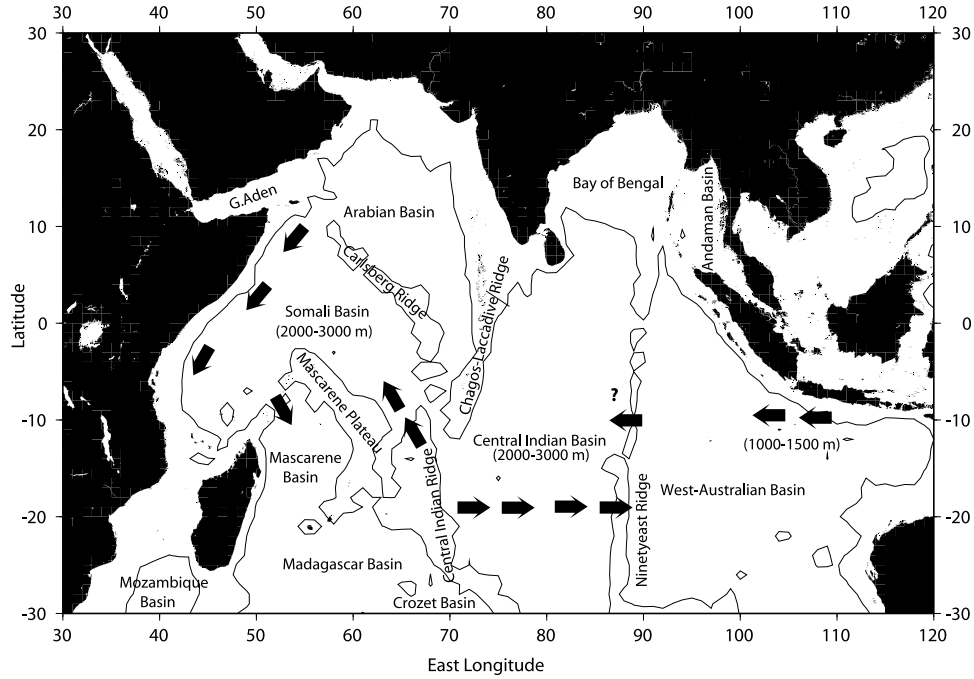

Figure 8. A schematic of the deep circulation pathways derived from the ^{3}He distribution. The inferred flow patterns are marked by arrows. The question mark over the westward flow at 10°S over the Ninetyeast Ridge denotes marginal evidence.

Indian Ocean the contribution of the Pacific and Indonesian Seas origin ^{3}He to the deep component of the Indonesian Throughflow must be known. It is likely that future studies will resolve this issue.

[38] Previous hydrographic and tracer studies have shown that in the Indian Ocean inflowing CDW is transformed into IDW and a portion of this IDW returns south between 2000 and 3500 m [*Warren* 1981; *Broecker et al.*, 1985]. The ^{3}He distribution supports the conclusion of these studies while pointing out additional pathways of deep water flow. The ^{3}He distribution presents a long-term averaged view and complements descriptions of flow obtained from snapshots of the density fields. The deep circulation scheme derived from the ^{3}He distribution is sketched in Figure 8 and is discussed below.

[39] In the western Indian Ocean, the ^{3}He distribution confirms a pathway for the southward flow of IDW from the northern Indian Ocean. In the deep Arabian Sea the data indicate a southwestward flow of IDW in the 2000–3000 m depth range close to the African Coast. The deep flow in this area has been the subject of considerable attention. A number of surveys in the area have shown differing properties at different times of the year suggesting flows seemingly aligned with the upper ocean monsoon winds [*Warren et al.*, 1966; *Fieux et al.*, 1986; *Schott et al.*, 1989; *Warren and Johnson*, 1992; *Beal et al.*, 2000; *Dengler et al.*, 2002]. *Warren and Johnson* [1992] applied the *Stommel and Arons* [1960] model to the deep water layer (2000–3500 m) in the Arabian Sea. In their model the upwelling from the bottom of the layer exceeded the upwelling from the top in order to sustain a southward flow in the layer. The resulting interior flow lines were directed southwestward and the model predicts a southwestward boundary current along the African Coast. The ^{3}He distribution is in good agreement with these results. It may not be possible to comment on the flow reversal with the ^{3}He data considering the range of the enrichment and the analytical uncertainties but the data do suggest that the mean flow is directed southwestward in this basin, which is consistent with other property distributions.

[40] IDW has been observed flowing southward at subtropical latitudes by a number of authors [e.g., *Warren* 1981; *Toole and Warren*, 1993]. On the basis of the ^{3}He distribution in the Arabian Sea, Amirante Passage and northern Mascarene Basin it is clear that some portion of the IDW found in the subtropical South Indian Ocean owes its origin to southward flow in the Arabian Sea and that it enters the South Indian Ocean via the Amirante Passage. Within the Amirante Passage, *Johnson et al.* [1998] found southward flow of IDW to be much larger than the northward flowing CDW beneath it. In a scheme where IDW is transformed CDW this results in a mismatch of volume fluxes in the Amirante Passage. Johnson et al. suggest that CDW upwelling in the eastern basins might flow westward north of the Amirante Passage at depths unconstrained by topography and join with the southward flow close to the African Coast which then flows south through the Amirante Passage. One possible pathway that supplies IDW to the Somali Basin is the westward flow into the Somali Basin that has been observed along the northeastern flank of the Mascarene Plateau [*Wyrtki*, 1971, *Warren* 1981, *Dengler et al.*, 2002]. This westward flow is observed in the ^{3}He distribution and it brings ^{3}He rich waters into the southeastern Somali Basin. Whereas it is possible that the westward inflow along the Mascarene Plateau contributes to the southward flow in the Amirante Passage, its pathway in the Somali Basin is not clear. As noted previously, there is a region of low-^{3}He anomaly between this helium enrichment and the ^{3}He enrichment farther west at the African Coast. It

is likely that this water mass is substantially modified before it reaches the western Somali Basin. These conclusions based on the ^{3}He distribution are similar to the conclusions made by *Dengler et al.* [2002] based on hydrographic data.

[41] In the Central Indian Basin an important result is evidence for prominent eastward flow in the south Indian Ocean. The eastward flow from the Central Indian Basin to the West Australian Basin deduced from the ^{3}He data confirms the recent discovery of eastward flow at 28°S over the saddles in the Ninetyeast Ridge by *Warren and Johnson* [2002]. A question raised in their study is whether the eastward flow upon entering the West Australian Basin turns north as a boundary current along the Ninetyeast Ridge and then returns to the Central Indian Basin through the westward flows at 10°S and 5°S saddles and further does this westward flow at 10°S contribute to the southward flow in the Amirante Passage via the boundary current observed along the northern flank of the Mascarene Plateau. The ^{3}He data do not resolve this question unambiguously but the ^{3}He distribution in the Central Indian Basin and at 8°S can be reconciled with this scenario.

[42] Another finding is the westward spreading ^{3}He signal in the intermediate layer in the eastern Indian Ocean. As noted previously this westward spreading is associated with the influx of Banda Sea Intermediate Water into the Indian Ocean. The Banda Sea Water has its origins in the intermediate waters of the Pacific Ocean and its presence in the Indian Ocean represents the deep component of the through flow between the Pacific and Indian Oceans [*Warren* 1981; *Gordon*, 1986; *Wijffels et al.*, 2002]. Observations suggest that the deep component may contribute a significant fraction of the total through flow [*Fieux et al.*, 1996; *Molcard et al.*, 1996; *Jean-Baptiste et al.*, 1997] while a coupled climate model study *Banks* [2000] suggests that the magnitude of deep through flow is dependent on the magnitude of the deep inflow into the Pacific and Indian Oceans. The ^{3}He data are likely to be a valuable tool for further study of the deep component of the through flow.

[43] In conclusion, this study presents an overview of a large helium data set in the Indian Ocean. The results point out new features with respect to the sources and deep circulation. The main points are summarized below:

[44] 1. The deep Indian Ocean receives significant ^{3}He input from sources located within and outside the Indian Ocean.

[45] 2. The measurements clearly map the extent of ^{3}He input from the previously known sources located in the Central Indian Ridge and at the Gulf of Aden and reveal new sources in the convergent margins in the eastern Indian Ocean.

[46] 3. The deep component of the through flow from the Pacific Ocean transports ^{3}He of deep Pacific and Indonesian Seas origin into the Indian Ocean.

[47] 4. The ^{3}He distribution reveals a deep eastward flow in the Central Indian Basin, in the 2000–3000 m depth range, which overflows into the West Australian Basin through the saddles in the Ninetyeast Ridge.

[48] 5. In the western Indian Ocean the ^{3}He distribution suggests southwestward flow of Indian Deep Water along the African Coast. Further, the data suggest that at least some of this water mass enters the south Indian Ocean through the Amirante Passage.

[49] 6. In the eastern Indian Ocean, the influx of Banda Sea Intermediate Waters causes ^{3}He enrichment in the 1000–1500 m depth range between 10°S and 12°S. The magnitude of the enrichment suggests a significant influx of this water mass.

[50] The WOCE data are likely to be used extensively in future studies. Further, as more of the Indian Ocean is mapped for hydrothermal activity, the source function will be better defined, resulting in a better resolved ^{3}He field and the implied deep flow.

[51] **Acknowledgments.** The authors greatly appreciate the comments of two anonymous reviewers whose careful reading and insightful comments significantly improved this manuscript. We thank the personnel who collected and processed the helium isotope data at UM, LDEO, PMEL and WHOI. National Science Foundation support is acknowledged for the UM part of the work through grants OCE-9820131 and OCE-998150. Support for the LDEO portion of the work was obtained from the National Science Foundation through awards OCE 94-13162 and OCE 98-20130. This is LDEO contribution number 6598.

References

Banks, H. T. (2000), Indonesian Throughflow in a coupled climate model and the sensitivity of the heat budget and deep overturning, *J. Geophys. Res.*, *105*(C11), 26,135–26,150.

Beal, L. M., R. L. Molinari, P. E. Robbins, and T. K. Chereskin (2000), Reversing bottom circulation in the Somali Basin, *Geophys. Res. Lett.*, *27*(16), 2565–2568.

Belviso, S., P. Jean-Baptiste, B. C. Nguyen, L. Merlivat, and L. Labeyrie (1987), Deep methane maxima and ^{3}He anomalies across the Pacific entrance to the Celebes Basin, *Geochim. Cosmochim. Acta*, *51*, 2673–2680.

Broecker, W. S., T. Takahashi, and T. Takahashi (1985), Source and flow patterns of deep ocean waters as deduced from potential temperature, salinity, and initial phosphate concentration, *J. Geophys. Res.*, *90*(C4), 6925–6939.

Clarke, W. B., W. J. Jenkins, and Z. Top (1976), Determination of tritium by mass spectrometric measurement of ^{3}He, *Int. J. Appl. Radiat. Isot.*, *27*, 515–522.

Coffin, M. F., L. M. Gahagan, and L. A. Lawver (1998), Present-day plate boundary digital data compilation, *Tech. Rep. 174*, 5 pp., Univ. of Texas Inst. for Geophys., Austin.

Condie, C. K. (1997), *Plate Tectonics and Crustal Evolution*, 279 pp., *Butterworth- Heinemann*, Woburn, Mass.

Craig, H., and J. E. Lupton (1981), Helium-3 and mantle volatiles in the ocean and oceanic crust, in *The Sea*, vol. 7, *The Oceanic Lithosphere*, edited by C. Emiliani, pp. 391–428, Wiley Interscience, Hoboken, N. J.

Dengler, M., D. Quadfasel, F. Schott, and J. Fischer (2002), Abyssal circulation in the Somali Basin, *Deep Sea Res., Part II*, *49*, 1297–1322.

Farley, K. A., E. Maier-Reimer, P. Schlosser, and W. S. Broecker (1995), Constraints on the mantle ^{3}He fluxes and deep-sea circulation from an oceanic general circulation model, *J. Geophys. Res.*, *100*(B3), 3829–3839.

Fieux, M., F. Schott, and J. C. Swallow (1986), Deep boundary currents in the western Indian Ocean revisited, *Deep Sea. Res., Part I*, *33*, 415–426.

Fieux, M., R. Molcard, and A. G. Ilahude (1996), Geostrophic transport of the Pacific-Indian Ocean throughflow, *J. Geophys. Res.*, *101*(C5), 12,421–12,432.

Fine, R. A. (1993), Circulation of Antarctic Intermediate Water in the South Indian Ocean, *Deep Sea Res., Part I*, *40*, 2021–2042.

Fisher, R. L., M. Z. Janstch, and R. L. Comer (1982), Scientific coordinators, sheet 5.05, Gen. Bathymetric Chart of the Oceans, Can. Hydrogr. Serv., Ottawa, Ont.

Gordon, A. L. (1986), Interocean exchange of thermocline water, *J. Geophys. Res.*, *91*(C4), 5037–5046.

Gordon, A. L., C. F. Giulivi, T. Takahashi, S. Sutherland, J. Morrison, and D. B. Olson (2002), Bay of Bengal nutrient-rich benthic layer, *Deep Sea Res., Part II*, *49*(7–8), 1411–1421.

Gordon, A. L., C. F. Giulivi, and A. G. Ilahude (2003), Deep topographic barriers within the Indonesian Seas, *Deep Sea Res., Part I*, *50*, 2205–2228.

Jamous, D., L. Memery, C. Andrie, P. Jean-Baptiste, and L. Merlivat (1992), The distribution of helium 3 in the deep western and southern Indian Ocean, *J. Geophys. Res.*, *97*(C2), 2243–2250.

Jean-Baptiste, P., S. Belviso, G. Alaux, B. C. Nguyen, and N. Milalopoulos (1990), ^{3}He and methane in the Gulf of Aden, *Geochem. Cosmochem. Acta*, *54*, 111–116.

Jean-Baptiste, P., F. Mantisi, L. Memery, and D. Jamous (1991), Helium-3 and CFC in the Southern Ocean: Tracers of water masses, *Mar. Chem.*, *35*(1/4), 137–150.

Jean-Baptiste, P., F. Mantisi, H. Pauwels, D. Grimaud, and P. Patriat (1992), Hydrothermal ^{3}He and manganese plumes at 19°29′S on the Central Indian Ridge, *Geophys. Res. Lett.*, *19*(17), 1787–1790.

Jean-Baptiste, P., M. Fieux, and A. G. Ilahude (1997), An eastern Indian Ocean ^{3}He section from Australia to Bali: Evidence for a deep Pacific-Indian throughflow, *Geophys. Res. Lett.*, *24*(21), 2577–2580.

Jenkins, W. B., and W. B. Clarke (1976), The distribution of ^{3}He in the western Atlantic Ocean, *Deep Sea Res., Part I*, *23*, 481–494.

Johnson, G. C., D. L. Musgrave, B. A. Warren, A. Ffield, and D. B. Olson (1998), Flow of bottom and deep water in the Amirante Passage and Mascarene Basin, *J. Geophys. Res.*, *103*(C13), 30,973–30,985.

Lott, D. E., III, and W. J. Jenkins (1998), Advances in analysis and shipboard processing of tritium and helium samples, *Int. WOCE Newsl.*, *30*, 27–30.

Ludin, A., R. Weppernig, G. Boenisch, and P. Schlosser (1998), Mass spectrometric measurement of helium isotopes and tritium, *Tech. Rep. 98-6*, Lamont-Doherty Earth Obs., Palisades, N. Y.

Lupton, J. E. (1998), Hydrothermal helium plumes in the Pacific Ocean, *J. Geophys. Res.*, *103*(C8), 15,853–15,868.

Lupton, J. E., and H. Craig (1980), Helium-3 in the western Indian Ocean (abstract), *Eos Trans. AGU*, *61*(46), 987.

Lupton, J. E., and H. Craig (1981), A major ^{3}He source at 15°S on the East Pacific Rise, *Science*, *214*, 13–18.

Mantyla, A. W., and J. L. Reid (1995), On the origins of deep and bottom waters in the Indian Ocean, *J. Geophys. Res.*, *100*(C2), 2417–2439.

Molcard, R., M. Fieux, and A. G. Ilahude (1996), The Indo-Pacific throughflow in the Timor Passage, *J. Geophys. Res.*, *101*(C5), 12,411–12,420.

Östlund, G. H., W. S. Broecker, H. Craig, and D. Spencer (1987), *GEOSECS Atlantic*, *Pacific and Indian Ocean Expedition*, vol. 7, *Shore-based Data and Graphics*, 199 plus xiv pp., Natl. Sci. Found., Washington, D. C.

Poisson, A., B. Schauer, and C. Brunet (1989), Les rapports des campaines a la mer a bord du "Marion Dufresne": MD49/Indigo-2, *Publ. 86-02*, 234 pp., Mission de Rech., terres australes et Antarct. Fr., Paris.

Reid, J. L. (2003), On the total geostrophic circulation of the Indian Ocean: Flow patterns, tracers, and transports, *Prog. Oceanogr.*, *56*(1), 137–186.

Rochford, D. (1966), Distribution of Banda Sea Intermediate water in the Indian Ocean, *Aust. J. Mar. Freshwater Res.*, *17*, 61–76.

Roether, W., R. Well, A. Putzka, and C. Ruth (1998), Component separation of oceanic helium, *J. Geophys. Res.*, *103*(C12), 27,931–27,946.

Rüth, C., R. Well, and W. Roether (2000), Primordial ^{3}He in the South Atlantic deep waters from sources on the Mid-Atlantic Ridge, *Deep Sea Res., Part I*, *47*, 1059–1075.

Schott, F., J. C. Swallow, and M. Fieux (1989), Deep currents underneath the equatorial Somali Current, *Deep Sea Res., Part I*, *36*, 1191–1199.

Smethie, W. M., Jr. (1993), Tracing the thermohaline circulation in the western North Atlantic using chloroflurocarbons, *Prog. Oceanogr.*, *31*, 51–99.

Spencer, D., W. S. Broecker, H. Craig, and R. F. Weiss (1982), *GEOSECS Indian Ocean Expedition*, vol. 6, *Sections and Profiles*, 140 plus xiv pp., Natl. Sci. Found., Washington, D. C.

Stommel, H., and A. B. Arons (1960), On the abyssal circulation of the world ocean—I, Stationary planetary flows patterns on a sphere, *Deep Sea Res., Part I*, *6*, 140–154.

Stuiver, M., P. D. Quay, and G. H. Ostlund (1984), Abyssal water carbon-14 distribution and the age of the world oceans, *Science*, *219*, 849–851.

Toole, J. M., and B. A. Warren (1993), A hydrographic section across the subtropical South Indian Ocean, *Deep Sea Res., Part I*, *40*, 1973–2019.

Toole, J. M., K. L. Polzin, and R. W. Schmitt (1994), Estimates of diapycnal mixing in the abyssal ocean, *Science*, *264*, 1120–1123.

Top, Z., W. B. Clarke, and W. J. Jenkins (1987), Tritium and primordial ^{3}He in the North Atlantic: A study in the region of Charlie Gibbs Fracture Zone, *Deep Sea Res., Part I*, *34*, 287–298.

Top, Z., A. Gordon, P. Jean-Baptiste, M. Fieux, and A. G. Ilahude (1997), ^{3}He in the Indonesian Seas: Inferences on deep pathways, *Geophys. Res. Lett.*, *24*(5), 547–550.

Warren, B. A. (1981), Trans-Indian hydrographic properties at lat. 18°S: Property distributions and circulation in the south Indian Ocean, *Deep Sea Res., Part I*, *28*, 759–788.

Warren, B. A. (1982), The deep water of the central Indian Basin, *J. Mar. Res.*, *40*, suppl., 823–860.

Warren, B. A., and G. C. Johnson (1992), Deep currents in the Arabian Sea in 1987, *Mar. Geol.*, *104*, 279–288.

Warren, B. A., and G. C. Johnson (2002), The overflows across the Ninetyeast Ridge, *Deep Sea Res., Part II*, *49*, 1423–1439.

Warren, B. A., H. Stommel, and J. C. Swallow (1966), Water masses and patterns of flow in the Somali Basin during the southwest monsoon of 1964, *Deep Sea Res., Part I*, *13*, 825–860.

Wijffels, S., J. Sprintall, M. Fieux, and N. Bray (2002), The JADE and WOCE I10/R6 throughflow sections in the southeast Indian Ocean. Part 1: Water mass distribution and variability, *Deep Sea Res., Part II*, *49*, 1341–1362.

Wyrtki, K. (1961), Scientific results of marine investigations of the South China Sea and the Gulf of Thailand 1959–1961, *NAGA Rep.* 2, 95 pp., Scripps Inst. of Oceanogr., Univ. of Calif., La Jolla.

Wyrtki, K. (1971), *Oceanographic Atlas of the International Indian Ocean Expedition*, U.S. Gov. Print. Off., Washington D. C., 531 pp.

R. Hohmann, Organe consultatif sur les Changements Climatiques, ProClim-, Bärenplatz 2, CH-3011 Bern, Switzerland.

M. Iskandarani, D. B. Olson, A. Srinivasan, and Z. Top, MPO Division, Rosenstiel School of Marine and Atmospheric Sciences, University of Miami, Miami, FL 33149, USA. (asrinivasan@rsmas.miami.edu)

W. J. Jenkins, Marine Geochemistry Department, Woods Hole Oceanographic Institution, Woods Hole, MA 02543, USA.

J. E. Lupton, Pacific Marine Environmental Laboratory, NOAA, Hatfield Marine Science Center, Newport, OR 97365, USA.

P. Schlosser, Lamont-Doherty Earth Observatory of Columbia University, Palisades, NY 10964, USA.